ISME

Transient Three-Dimensional Thermal Analysis of a Slab with Internal Heat Generation and Heated by a Point Moving Heat Source

M. G Sobamowo *
Assistant Professor

L. O. Jayesimi†
Instructor

M. A. Waheed‡
Professor

In this work, analysis of transient three-dimensional heat transfer in a slab with internal heat generation and heated by a point moving heat source along its axis is carried out using integral transforms methods. The heat input into slab or workpiece by the moving heat source is considered in the model. From the results, it was established that the temperature of the material during the heat transfer process decreases while the time required to reach the peak temperature increases with increasing distance from the centerline. Also, the rate of heating and the rate of cooling decrease with increasing distance from the centerline. The computed results at different monitoring locations show typical features of the temperature profiles and they afford a close analysis of the factors governing the heat flow in a point moving heat source.

Keywords: Transient heat transfer; Three-dimensional model; Point Moving heat source; Integral transforms; Analytical solutions.

1 Introduction

Heat transfer process is one of the most important aspects in engineering and scientific studies of materials behaviours. A good understanding of heat transfer processes in material is helpful in predicting the thermal cycles in the material under thermal applications and processes also in evaluating the thermal and temperature-dependent properties of the materials. The temperature profile and the rate of cooling at and near the surface of a material can affect the metallurgical properties, microstructures, thermal shrinkage, thermal cracking, hardness distribution, residual stresses and heat affected zones of the material [1]. Therefore, the determination of temperature distribution helps to minimize the thermal related problems. Also, temperature measurements during the manufacturing process of a moving coordinate system such as welding are very difficult to achieve because of the intense plastic deformation produced by the rotation and translation of the tool.

*Assistant Professor, Corresponding Author, Department of Mechanical Engineering, University of Lagos, Akoka, Lagos, Nigeria, mikegbeminiyi@gmail.com
† Instructor, Works and Physical Planning Department, University of Lagos, Akoka, Lagos, Nigeria, lawrence@unilag.edu.ng
‡ Professor, Department of Mechanical Engineering, Federal University of Agriculture, Abeokuta, Nigeria, gsobomwo@unilag.edu.ng

Moreover, thermal analysis of manufacturing process can be used predict the transient temperature field, maximum temperatures, active thermal stress and forces and may be extended to determine the residual stress in the joint. The effect of process temperature on material, particularly when it is too high, can lead to rapid tool wear, thermal flaking, creep and fracturing due to thermal shocks, dimensional inaccuracy of the material in process due to thermal distortion and expansion-contraction during and after manufacturing process, surface damage by oxidation, rapid corrosion and burning etc.

Also, temperature variations and flow patterns in a workpiece during heat processes are important to engineers for an appropriate designing of manufacturing process layout. Consequently, it is important to obtain information about the temperature distribution during the processes either by numerical or analytical methods.

However, the nonlinearities and the complexities in most developed models of the moving heat source problems or moving coordinate systems have made it very difficult to develop exact analytical solutions which provide good physical insights into the significance of various parameters affecting the processes. Consequently, recourse has always been made to numerical methods in solving the problems. However, from comparatively simple analytical solutions, it is possible to build up more complex solutions to describe different situations and conditions at the surface of the workpiece. In various ways, it is possible to solve more complicated problems in terms of these simple analytical solutions, an approach that can lead to better understanding before resorting to more complicated computational methods [2].

Therefore, the classical way for finding exact analytical solution is obviously still very important since it serves as an accurate benchmark for numerical solutions. Also, the experimental data are useful to access the mathematical models, but are never sufficient to verify the numerical solutions of established mathematical models. Comparison between the numerical calculations and experimental data often fail to reveal the compensation of modelling deficiencies through the computational errors or unconscious approximations in establishing applicable numerical schemes. Additionally, exact analytical solutions for specified problems are essential for the development of efficient applied numerical simulation tools. Inevitably, exact analytical expressions are required to show the direct relationship between the models parameters. When such exact analytical solutions are available, they provide good insights into the significance of various system parameters affecting the phenomena as it gives continuous physical insights into the problems than pure numerical or computation methods. Furthermore, most of the analytical approximation and purely numerical methods that were applied in literatures to nonlinear problems are computationally intensive.

Exact analytical expression is more convenient for engineering calculations compare with experimental or numerical studies and it is obvious starting point for a better understanding of the relationship between physical quantities/properties. It is convenient for parametric studies, accounting for the physics of the problem. It appears more appealing than the numerical solution as it helps to reduce the computation costs, simulations and task in the analysis of real life problems. Therefore, the need for such exact analytical solutions in the analysis of moving heat source problems in many metallurgical processes such welding, surface hardening or continuous casting cannot be overemphasized.

However, the theory of heat flow due to a moving source has received little attention in the study of the general treatment of heat flow in metals. Rosenthal and Cameron [3, 4] made the first attempt by applying instantaneous point source solution in presenting the exact theory of moving point heat source in arc welding process while Weichert and Schonert [5] presented a series of studies concerning the temperature rise near a moving heat source.

However, these studies were limited to the linear and steady-state heat transfer. Such steady state heat transfer analysis makes the temperature field appear invariant to an observer moving along with the heat source, at the same speed.

In most cases and unfortunately, the solution is too complicated for direct practical applications [6]. Therefore, several attempts, both experimental and theoretical, have been made to describe the temperature situations created by moving heat source. Kim [6] presented one-directional analytical solution to heat conduction problems in solid with a moving heat source using Fourier series. Carslaw and Jaeger [7] adopted Green's function and method of images to develop analytical solutions of moving heat source problems. Dowden *et al.* [2] developed a simple model for time-dependent line and point sources in welding processes. Malmuth [8] analyzed temperature field of a moving point-source problem with change of state while Grosh*et al.* [9] pointed properties heated by moving heat source and in recent times, Kuang and Atluri [10] applied a moving mesh finite element method to determine the temperature field due to a moving heat Source. Webb and Viskanta [11] investigated the heat transfer during melting the pure metal from an isothermal vertical wall using finite different method.
However, the theoretical analysis of temperature distribution around moving source shows singularity at the locus of the heat source. Although, the restriction is not severe for great distances from the source, for distances comparable with the real source size, the results become incorrect [6]. Jeager [12] used the instantaneous point source solution to find the temperature distribution due to a moving heat source within an infinite body. The same method was applied by Peak and Gagliano [13] to determine the transient temperature distribution for laser drilled holes in ceramic substrate materials.
In their work, a circular heat source was considered and a temperature profile was formed in terms of double integrals, which cannot be solved analytically. Also, the same approach has been used by Zubair and Chaudhry [14] for a moving line source with time variable heat flow rate, and Terauchi *et al.* [15] for moving circular and rectangular plane sources where the effect of different heat flux distributions has been investigated for the quasi-steady condition. Combining the asymptotic solutions of very fast moving, and stationary heat sources, Muzychka and Yovanovich [16] developed a model to predict the thermal resistance of non-circular moving heat sources. Their solution is only valid for quasi-steady condition. Recently, Houand Komandouri [1] used point source solution in the quasi-steady condition to present a general solution for transient temperature distribution of a moving plane source in a half space. Their solution includes a triple integral which they solved numerically for various heat source shapes including elliptic, circular, rectangular and square surfaces.
More recently, using almost the same method, Kou and Lin [17] developed a three dimensional solution for the rectangular shaped moving heat source for surface grinding while Nyugen*et al.* [18] presented three-dimensional analytical solutions for a double-ellipsoidal power density moving heat source in a semi-infinite body using the same point source solution. Several attempts have been made by other researchers to analyze the problems [19-39]. However, most of the previous solutions assumed that heat transfer to or by the moving heat source can be neglected. However, the ratio of the heat transfer to the heat source or tool was estimated to be up to 20% by some researchers. The condition that there is no additional heat input to the slab or the workpiece imposes a restriction on the accurate determination of the heat distribution in the workpiece. In order to model the heat transfer process accurately, it is necessary to include the heat generated by the tool in the modeling. Therefore, a better predictive model is required. Although, both experimental procedures and mathematical models in limited dimensional coordinates have been utilized to understand material behavior during manufacturing process, three-dimensional modeling is very much important for detail analysis and understanding of the manufacturing processes. Also, the analytical solutions of such three-dimensional models are very much more important.
Therefore, in this work, analytical solutions for transient three-dimensional temperature distributions in a slab with internal heat generation subjected to moving heat source at a constant

speed along its axis is carried out using integral transforms methods (Laplace and Fourier transforms methods).
The physical significance of the integral transforms methods facilitates observation of great many properties and hidden views, of both mathematical and physical interests which are not yet very well-known and have not met with proper appreciations. The result of the passage of the heat source shows that the rise of temperature produced at a given near the source tends to become constant.

2 Problem Formulation and Analytical Solutions

Figure (1) shows a three-dimensional rectangular coordinate system with a moving heat source such as found in welding, surface hardening, laser cutting, milling process, continuous casting and tribological applications. The moving heat source which is independent of time, generates heat at a rate given by Q_P. The heated zone starts from the right end of the bar and begins to move toward the left at a constant axial velocity *u* along the slab.
Assuming the tool material is isotropic and homogeneous, the thermal properties of the material are independent of temperature, no phase change occurs during the process, thermal boundary conditions are symmetrical across the manufacturing process centerline and heat transfer from the workpiece to the clamp is negligible, then the governing equation for the process is given by Eq.(1).

$$\frac{\partial T}{\partial t}=\alpha\left(\frac{\partial^2 T}{\partial x^2}+\frac{\partial^2 T}{\partial y^2}+\frac{\partial^2 T}{\partial z^2}\right)+Q_{slab/workpiece}\frac{A_r}{\rho c_p V} \tag{1}$$

Where $\alpha=\dfrac{k}{\rho c_p}$, A_r is an arbitrary selected area on the tool, *V* is the volume over which the heat the heat generated on A_r is dissipated and the term $Q_{wor\ k}$ is the rate of internal heat generation per unit volume of the slab/workpiece associated with the process and accounts for the boundary conditions

2.1 Initial and Boundary Conditions

$$\text{Initial condition: } t = 0,\ \ T(x,y,z)=T_o \tag{2}$$

2.2 Boundary Conditions

The heat flux boundary condition at the moving heat source-slab interface

$$-k\left.\frac{\partial T}{\partial z}\right|_{z=0}=\gamma Q_p,\quad \textit{in the range } R_p\le r\le R_s \tag{3}$$

Where γ is the fraction of heat partitioned to the slab/workpiece.

$$\gamma=\frac{\sqrt{(k\rho c_p)_{slab/workpiece}}}{\sqrt{(k\rho c_p)_{slab/workpiece}}+\sqrt{(k\rho c_p)_{heat\ source/tool}}}$$

For the point moving heat source under investigation, term $Q_{slab/workpiece}$ has been taken to be invariant of *x* and *y*.

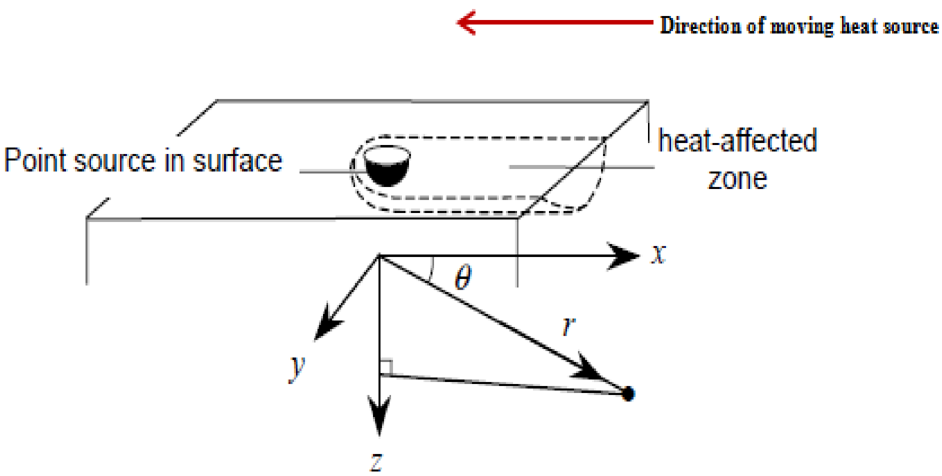

Figure 1 Point source on the surface of the workpiece [11].

$$-k\frac{\partial T}{\partial z}\bigg|_{z=0} = h(T - T_\infty) + \sigma\varepsilon(T^4 - T_\infty^4) \tag{4}$$

At the top surface beyond the shoulder, the boundary condition for heat exchange between the top surface of the workpiece and the surrounding involved convective and radiative boundary condition.

Where the effective heat transfer coefficient

$$h_{eff} = h + \sigma\varepsilon\left(T^3 + T_\infty T^2 + T_\infty^2 T + T_\infty^3\right) \tag{5}$$

Consequently, the boundary conditions in Eq. (4) becomes,

$$-k\frac{\partial T}{\partial z}\bigg|_{z=0} = h_{eff}(T - T_\infty), \quad r \geq R_s \tag{6}$$

The heat loss from the bottom surface is practically heat conduction from workpiece and support base presents difficulty in modeling. To circumvent the problem and simplify the analysis, a high overall heat transfer coefficient was assured. The heat loss was model approximately by using heat flux by convection q_b

$$-k\frac{\partial T}{\partial z}\bigg|_{z=d} = \beta_b(T - T_\infty) \tag{7}$$

All other boundary conditions at ambient temperature which means

$$T\big|_{y=-\infty} = T_\infty \; T\big|_{y=\infty} = T_\infty \; T\big|_{x=-\infty} = T_\infty \; T\big|_{x=\infty} = T_\infty \tag{8}$$

In order to write the governing energy equation, the initial and the conditions in simpler and standard forms with fewer parameters so as to avoid errors in the analysis, ease the solution procedures as the equation and the conditions are transformed to standard forms and bring out dimensionless number controlling the processes as this will aid in further analysis (such as sensitivity and scale analysis) of the processes and the system, the following dimensionless parameters are used to non-dimensionalize the governing equations, the initial and boundary conditions.

$$\theta=\frac{T-T_\infty}{T_o-T_\infty},\quad X=\frac{x}{d},\quad Y=\frac{y}{d},\quad Z=\frac{z}{d},\quad \tau=\frac{\alpha t}{d^2},\quad \dot{Q}_p=\frac{\gamma Q_p d}{(T_o-T_\infty)k_w},\quad \overline{R}=\frac{r}{R}$$
$$Bi_{bc}=\frac{\beta_{bc}d}{k},\quad Bi_{eff}=\frac{h_{eff}d}{k},\quad \dot{Q}'''_{work}=\frac{\alpha t A_r Q_{slab/workpiece}}{\rho c_p V(T_o-T_\infty)d^2} \tag{9}$$

Applying the dimensionless parameters to Eqs. (1), (2), (3), (6), (7) and (8), we arrived at the non-dimensionalized forms of Eqs. (1) as

$$\frac{\partial\theta}{\partial\tau}=\frac{\partial^2\theta}{\partial X^2}+\frac{\partial^2\theta}{\partial Y^2}+\frac{\partial^2\theta}{\partial Z^2}+\dot{Q}'''_{work} \tag{10}$$

2.3 Initial condition:

$$\tau=0,\ \ \theta(X,Y,Z)=1 \tag{11}$$

2.4 Boundary Conditions

The heat flux boundary condition at the tool-workpiece interface

$$\left.\frac{\partial\theta}{\partial Z}\right|_{Z=0}=\dot{Q}_p,\quad \textit{in the range } \overline{R}_p\le\overline{R}\le\overline{R}_s \tag{12}$$

$$\left.\frac{\partial\theta}{\partial Z}\right|_{Z=0}=-Bi_{eff}\theta,\quad \overline{R}\ge\overline{R}_s \tag{13}$$

Also,

$$\left.\frac{\partial\theta}{\partial Z}\right|_{Z=1}=-Bi_{bc}\theta, \tag{14a}$$

$$\left.\theta\right|_{Y=-\infty}=0\quad \left.\theta\right|_{Y=\infty}=0\quad \left.\theta\right|_{X=-\infty}=0\quad \left.\theta\right|_{X=\infty}=0 \tag{14b}$$

Applying Laplace transform to Eq. (10)

$$s\overline{\theta}-1=\frac{\partial^2\overline{\theta}}{\partial X^2}+\frac{\partial^2\overline{\theta}}{\partial Y^2}+\frac{\partial^2\overline{\theta}}{\partial Z^2}+\frac{Q'''_{work}}{s} \tag{15}$$

Also, applying generalized finite Fourier transform on space Z-domain

$$s\tilde{\bar{\theta}}(\beta_m,Y,Z,s)-\tilde{1}=\frac{\partial^2\tilde{\bar{\theta}}(\beta_m,Y,Z,s)}{\partial X^2}+\frac{\partial^2\tilde{\bar{\theta}}(\beta_m,Y,Z,s)}{\partial Y^2}+\frac{\tilde{Q}'''_{work}}{s}-\beta_m{}^2\tilde{\bar{\theta}}(\beta_m,Y,Z,s)$$
$$+\left[\frac{\partial\bar{\theta}(X,Y,Z,s)}{\partial X}+Bi_{eff}\bar{\theta}\right]_{Z=1}-\left[\frac{\partial\bar{\theta}(X,Y,Z,s)}{\partial X}-Bi_{eff}\bar{\theta}\right]_{Z=0} \tag{16}$$

After the applications of the boundary conditions in Eqs. (12), (13) and (14), the above Eq. (16) reduces to

$$\frac{\partial^2\tilde{\bar{\theta}}(\beta_m,Y,Z,s)}{\partial X^2}+\frac{\partial^2\tilde{\bar{\theta}}(\beta_m,Y,Z,s)}{\partial Y^2}-(s+\beta_m{}^2)\tilde{\bar{\theta}}(\beta_m,Y,Z,s)=-\tilde{1}-\frac{\tilde{Q}'''_{work}}{s} \tag{17}$$

In order to amend the solution to practical solution, it is established that a solution for $\tilde{\bar{\theta}}$ that depends only on the radial distance from the origin, $\bar{R}=\sqrt{X^2+Y^2}$ is sought after. In that case, using chain rule in Eq. (17), one arrives at

$$\frac{\partial^2\tilde{\bar{\theta}}}{\partial X^2}=\frac{1}{\bar{R}}\frac{\partial\tilde{\bar{\theta}}}{\partial\bar{R}}+\frac{X^2}{\bar{R}^2}\left(\frac{\partial^2\tilde{\bar{\theta}}}{\partial\bar{R}^2}\right)-\frac{X^2}{\bar{R}^3}\frac{\partial\tilde{\bar{\theta}}}{\partial\bar{R}} \tag{18}$$

Similarly

$$\frac{\partial^2\tilde{\bar{\theta}}}{\partial Y^2}=\frac{1}{\bar{R}}\frac{\partial\tilde{\bar{\theta}}}{\partial\bar{R}}+\frac{Y^2}{\bar{R}^2}\left(\frac{\partial^2\tilde{\bar{\theta}}}{\partial\bar{R}^2}\right)-\frac{Y^2}{\bar{R}^3}\frac{\partial\tilde{\bar{\theta}}}{\partial\bar{R}} \tag{19}$$

On substituting Eqs. (18) and Eq. (19) into Eq. (17), it was given that

$$\frac{1}{\bar{R}}\frac{\partial\tilde{\bar{\theta}}}{\partial\bar{R}}+\frac{X^2}{\bar{R}^2}\left(\frac{\partial^2\tilde{\bar{\theta}}}{\partial\bar{R}^2}\right)-\frac{X^2}{\bar{R}^3}\frac{\partial\tilde{\bar{\theta}}}{\partial\bar{R}}+\frac{1}{\bar{R}}\frac{\partial\tilde{\bar{\theta}}}{\partial\bar{R}}+\frac{Y^2}{\bar{R}^2}\left(\frac{\partial^2\tilde{\bar{\theta}}}{\partial\bar{R}^2}\right)-\frac{Y^2}{\bar{R}^3}\frac{\partial\tilde{\bar{\theta}}}{\partial\bar{R}}$$
$$-(s+\beta_m{}^2)\tilde{\bar{\theta}}(\beta_m,Y,Z,s)=-\tilde{1}-\frac{\tilde{Q}'''_{work}}{s} \tag{20}$$

Which reduces to

$$\frac{d^2\tilde{\bar{\theta}}(\beta_m,\bar{R},s)}{d\bar{R}^2}+\frac{1}{\bar{R}}\frac{d\tilde{\bar{\theta}}(\beta_m,\bar{R},s)}{d\bar{R}}-(s+\beta_m{}^2)\tilde{\bar{\theta}}(\beta_m,\bar{R},s)=-1-\frac{\tilde{Q}'''_{work}}{s} \tag{21}$$

The complementary solution of Equ. (21) is given as

$$\tilde{\bar{\theta}}_C(\beta_m,\bar{R},s)=AI_0\left[\sqrt{(s+\beta_m{}^2)}\bar{R}\right]+BK_o\left[\sqrt{(s+\beta_m{}^2)}\bar{R}\right] \tag{22}$$

Where I_0 and K_o are the modified Bessel functions of the first and second kind of order zero.

The particular integral of Equ. (21) is given as

$$\tilde{\bar{\theta}}_{PI}(\beta_m,\bar{R},s)=\frac{\tilde{Q}'''_{work}}{s(s+\beta_m{}^2)}+\frac{\tilde{1}}{(s+\beta_m{}^2)} \tag{23}$$

Therefore, the complete solution of Equ. (21) is

$$\tilde{\bar{\theta}}(\beta_m,\bar{R},s)=AI_0\left[\sqrt{(s+\beta_m{}^2)\bar{R}}\right]+BK_o\left[\sqrt{(s+\beta_m{}^2)\bar{R}}\right]+\frac{\tilde{Q}'''_{work}}{s(s+\beta_m{}^2)}+\frac{\tilde{1}}{(s+\beta_m{}^2)} \tag{24}$$

In order to make use of this solution in Eq. (24), it is helpful to understand the characteristics of the two modified Bessel functions of the first and second kind of order zero. I_o increases indefinitely as R increases and K_o tends to zero as R increases.
For large values of R, the asymptotic forms of the Bessel functions give the solution as

$$\tilde{\bar{\theta}}(\beta_m,\bar{R},s)=\frac{A}{\sqrt[4]{(s+\beta_m{}^2)}\sqrt{2\pi\bar{R}}}exp\left[\sqrt{(s+\beta_m{}^2)\bar{R}}\right]+\frac{B\pi}{\sqrt[4]{(s+\beta_m{}^2)}\sqrt{2\pi\bar{R}}}exp\left[-\sqrt{(s+\beta_m{}^2)\bar{R}}\right]+\frac{\tilde{Q}'''_{work}}{s(s+\beta_m{}^2)}+\frac{\tilde{1}}{(s+\beta_m{}^2)} \tag{25}$$

As $\bar{R}>0$, the coefficient of A tends to infinity as $\bar{R}$ tends to infinity far downstream of the heat source. Since this is inconsistent with the normal conditions of the problem under investigation, the coefficient A must be zero. Therefore, Equ. (25) reduces to

$$\tilde{\bar{\theta}}(\beta_m,\bar{R},s)=\frac{B\pi}{\sqrt[4]{(s+\beta_m{}^2)}\sqrt{2\pi\bar{R}}}exp\left[-\sqrt{(s+\beta_m{}^2)\bar{R}}\right]+\frac{\tilde{Q}'''_{work}}{s(s+\beta_m{}^2)}+\frac{\tilde{1}}{(s+\beta_m{}^2)} \tag{26}$$

Resolving into partial fraction, Eq. (26) becomes

$$\tilde{\bar{\theta}}(\beta_m,\bar{R},s)=\frac{B\pi}{\sqrt[4]{(s+\beta_m{}^2)}\sqrt{2\pi\bar{R}}}exp\left[-\sqrt{(s+\beta_m{}^2)\bar{R}}\right]+\frac{\tilde{Q}'''_{work}}{\beta_m{}^2}\left[\frac{1}{s}-\frac{1}{s+\beta_m{}^2}\right]+\frac{\tilde{1}}{(s+\beta_m{}^2)} \tag{27}$$

The next step is the application of inverse Laplace transform to the above Eq. (27). Although, it is a trivial issue to find the inverse Laplace transforms of the second and the third terms in the RHS of the equation, the inverse Laplace transforms of the first term in the RHS of Eq. (27) proves somehow not straight-forward and nontrivial. However, with the use of convolution theorem as shown in the proceeding analysis, helps in establishing the required inverse Laplace transform.
Let the first term in Eq. (27) be given as $\tilde{\bar{M}}(\beta_m,\bar{R},s)$, i.e.

$$\tilde{\bar{M}}(\beta_m,\bar{R},s)=\frac{B\pi}{\sqrt{2\pi\bar{R}}}\frac{exp\left[-\sqrt{(s+\beta_m{}^2)\bar{R}}\right]}{\sqrt[4]{(s+\beta_m{}^2)}} \tag{28}$$

The above Eq. (28) could be written as

$$\tilde{\tilde{M}}(\beta_m,\bar{R},s)=\frac{B\pi}{\sqrt{2\pi\bar{R}}}exp\left[-\sqrt{(s+\beta_m{}^2)}\bar{R}\right]\left[\frac{1}{\sqrt[4]{(s+\beta_m{}^2)}}\right]=\Omega(\beta_m,\bar{R},s)\Psi(s) \tag{29}$$

Where

$$\Omega(\beta_m,\bar{R},s)=\left[exp\left[-\sqrt{(s+\beta_m{}^2)}\bar{R}\right]\right] \qquad \Psi(s)=\frac{B\pi}{\sqrt{2\pi\bar{R}}}\frac{1}{\sqrt[4]{(s+\beta_m{}^2)}}$$

The inverse Laplace transform of $\Omega(\beta_m,R,s)$ is given as

$$L^{-1}\left[\Omega(\beta_m,\bar{R},s)\right]=L^{-1}\left[exp\left[-\sqrt{(s+\beta_m{}^2)}\bar{R}\right]\right] \tag{30}$$

i.e.

$$L^{-1}\left[\Omega(\beta_m,\bar{R},s)\right]=\frac{1}{2\sqrt{\pi\tau^3}}exp\left[-\left(\beta_m^2\tau+\frac{\bar{R}^2}{4\tau}\right)\right] \tag{31}$$

While the inverse Laplace transform of $\Psi(s)$ is given as

$$\Psi(s)=\frac{B\pi}{\sqrt{2\pi\bar{R}}}L^{-1}\left[\frac{1}{\sqrt[4]{(s+\beta_m{}^2)}}\right]=\frac{B}{\sqrt{2\pi^{\frac{1}{4}}\bar{R}\tau^{\frac{3}{2}}}}exp(-\beta_m^2\tau) \tag{32}$$

By convolution theorem,

$$L^{-1}[\tilde{\tilde{M}}(\beta_m,\bar{R},s)]=L^{-1}\left\{\frac{B\pi}{\sqrt{2\pi\bar{R}}}\frac{exp\left[-\sqrt{(s+\beta_m{}^2)}\bar{R}\right]}{\sqrt[4]{(s+\beta_m{}^2)}}\right\}=\left\{\frac{B}{\pi}\frac{1}{\bar{R}}exp\left\{-\left[\left(\beta_m^2\tau+\frac{\bar{R}^2}{4\tau}\right)\right]\right\}\right\} \tag{33}$$

Therefore, the inverse Laplace transform of Eq. (27) is given as

$$\begin{aligned}\tilde{\theta}(\beta_m,\bar{R},\tau)=&\left\{\frac{B}{\pi}\frac{1}{\bar{R}}exp\left\{-\left[\left(\beta_m^2\tau+\frac{\bar{R}^2}{4\tau}\right)\right]\right\}\right\}\\&+\frac{\tilde{Q}'''_{work}}{\beta_m{}^2}\left[1-exp(-\beta_m{}^2\tau)\right]+[\tilde{1}\times exp(-\beta_m{}^2\tau)]\end{aligned} \tag{34}$$

The constant B in the above equation is found from Q_p, which is the energy input into the slab/workpiece from the translation, rotation, and downward forces i.e. total heat input from the heating source. Repenting the point moving heat source roughly by a row of line sources over the segment $-l<x<+l$. If the total power per unit depth is Q_P/w.

$$\begin{aligned}\tilde{\theta}(\beta_m,\bar{R},\tau)=&\left\{\left\{\frac{Q_p}{2\pi\bar{R}}exp\left\{-\left[\left(\beta_m^2\tau+\frac{\bar{R}^2}{4\tau}\right)\right]\right\}\right\}\right\}\\&+\frac{\tilde{Q}'''_{work}}{\beta_m{}^2}\left[1-exp(-\beta_m{}^2\tau)\right]+[\tilde{1}\times exp(-\beta_m{}^2\tau)]\end{aligned} \tag{35}$$

Applying inverse finite Fourier transform to Eq. (35), one arrives at

$$\theta(Z,\bar{R},\tau)=\frac{Q_p}{2\pi\bar{R}}\sum_{m=0}^{\infty}\frac{\left(\beta_m^2+\beta_{bc}^2\right)\begin{bmatrix}cos(\beta_m Z)\\ +Bi_{eff}sin(\beta_m Z)\end{bmatrix}\left\{\begin{array}{l}\left\{exp\left\{-\left[\left(\beta_m^2\tau+\dfrac{\bar{R}^2}{4\tau}\right)\right]\right\}\right\}\\ +\dfrac{2\pi R\tau}{Q_p}\left\{\begin{array}{l}\dfrac{\tilde{Q}'''_{work}}{\beta_m{}^2}\left[1-exp(-\beta_m{}^2\tau)\right]\\ +[\tilde{1}\times exp(-\beta_m{}^2\tau)]\end{array}\right\}\end{array}\right\}}{\left(\beta_m^2+Bi_{eff}^2\right)\left\{\begin{array}{l}\left[(\beta_m^2+\beta_{bc}^2)+\beta_{bc}\right]\\ +Bi_{eff}(\beta_m^2+\beta_{bc}^2)\end{array}\right\}} \tag{36}$$

The above Eq. (36) can also be written as

$$\theta(Z,\bar{R},\tau)=\frac{Q_p}{2\pi\bar{R}}exp\left\{-\left[\left(\frac{\bar{R}^2}{4\tau}\right)\right]\right\}\sum_{m=0}^{\infty}\frac{\left(\beta_m^2+\beta_{bc}^2\right)\begin{bmatrix}cos(\beta_m Z)\\ +Bi_{eff}sin(\beta_m Z)\end{bmatrix}\left\{\begin{array}{l}\left\{exp\left\{-\left[\left(\beta_m^2\tau\right)\right]\right\}\right\}\\ +\dfrac{2\pi R}{Q_p}\left\{\begin{array}{l}\dfrac{\tilde{Q}'''_{work}}{\beta_m{}^2}\left[1-exp(-\beta_m{}^2\tau)\right]\\ +[\tilde{1}\times exp(-\beta_m{}^2\tau)]\end{array}\right\}\end{array}\right\}}{\left(\beta_m^2+Bi_{eff}^2\right)\left\{\begin{array}{l}\left[(\beta_m^2+\beta_{bc}^2)+\beta_{bc}\right]\\ +Bi_{eff}(\beta_m^2+\beta_{bc}^2)\end{array}\right\}} \tag{37}$$

Where β_m are the positive roots of $tan\beta_m=\dfrac{\beta_m(Bi_{eff}+\beta_{bc})}{\beta_m^2-Bi_{eff}\beta_{bc}}$

and

$$\tilde{Q}'''_{work}=\int_0^1\left[\beta_m cos(\beta_m Z)+Bi_{eff}sin(\beta_m Z)\right]\tilde{Q}'''_{work}dZ=Q'''_{work}\left[sin\beta_m+\frac{Bi_{eff}}{\beta_m}(1-cos\beta_m)\right]$$

$$\tilde{1}=\int_0^1\left[\beta_m cos(\beta_m Z)+Bi_{eff}sin(\beta_m Z)\right]dZ=\left[sin\beta_m+\frac{Bi_{eff}}{\beta_m}(1-cos\beta_m)\right] \tag{38}$$

For the case where the heat generated in the work is neglected and the initial temperature of the workpiece is the same as the atmospheric, it is given as

$$\theta(Z,\bar{R},\tau)=\frac{Q_p}{2\pi\bar{R}}exp\left\{-\left[\left(\frac{\bar{R}^2}{4\tau}\right)\right]\right\}\sum_{m=0}^{\infty}\frac{(\beta_m^2+\beta_{bc}^2)[cos(\beta_m Z)+Bi_{eff}sin(\beta_m Z)]\left\{\left\{exp\left\{-\left[\left(\beta_m^2\tau\right)\right]\right\}\right\}\right\}}{\left(\beta_m^2+Bi_{eff}^2\right)\left\{\left[(\beta_m^2+\beta_{bc}^2)+\beta_{bc}\right]+Bi_{eff}(\beta_m^2+\beta_{bc}^2)\right\}} \tag{39}$$

For the case where the temperature at a point $P(X_, Y_, Z)$ at time *t* in the infinite plate subjected to an instantaneous point heat source of intensity Q_P at point $P'(X'_, Y'_, 0)$ at time τ' is found as

$$\theta(Z,\bar{R},\tau)=\frac{Q_p}{2\pi\bar{R}}exp\left\{-\left[\left(\frac{(X-X')^2+(Y-Y')^2}{4(\tau-\tau')}\right)\right]\right\}\sum_{m=0}^{\infty}\frac{\begin{Bmatrix}(\beta_m^2+\beta_{bc}^2)[cos(\beta_m Z)\\+Bi_{eff}sin(\beta_m Z)]\end{Bmatrix}\begin{Bmatrix}\left\{exp\left\{-\left[\left(\beta_m^2(\tau-\tau')\right)\right]\right\}\right\}\\+\dfrac{2\pi R}{Q_p}\begin{Bmatrix}\dfrac{\tilde{Q}'''_{work}}{\beta_m{}^2}\left[1-exp(-\beta_m{}^2(\tau-\tau')\right]\\+[\tilde{1}\times exp(-\beta_m{}^2(\tau-\tau')]\end{Bmatrix}\end{Bmatrix}}{\left\{\left(\beta_m^2+Bi_{eff}^2\right)\left\{\left[(\beta_m^2+\beta_{bc}^2)+\beta_{bc}\right]+Bi_{eff}(\beta_m^2+\beta_{bc}^2)\right\}\right\}} \tag{40}$$

When the heat generated in the work is neglected as in previous researches and when the initial temperature of the workpiece is the same as the atmospheric, one arrives at

$$\theta(Z,\bar{R},\tau)=\frac{Q_p}{2\pi\bar{R}}exp\left\{-\left[\left(\frac{\bar{R}^2}{4(\tau-\tau')}\right)\right]\right\}\sum_{m=0}^{\infty}\frac{\begin{Bmatrix}(\beta_m^2+\beta_{bc}^2)[cos(\beta_m Z)\\+Bi_{eff}sin(\beta_m Z)]\end{Bmatrix}\left\{\left\{exp\left\{-\left[\left(\beta_m^2(\tau-\tau')\right)\right]\right\}\right\}\right\}}{\left\{\left(\beta_m^2+Bi_{eff}^2\right)\left\{\left[(\beta_m^2+\beta_{bc}^2)+\beta_{bc}\right]+Bi_{eff}(\beta_m^2+\beta_{bc}^2)\right\}\right\}} \tag{41}$$

In many problems of material processing it is extremely convenient to use a coordinate system that is fixed with respect to the power source. The reason is that after a time, conditions may become quasi-steady if the power of the source remains constant. In such a coordinate system, any function of the coordinate vector R and time τ *is* the value of the function at that particular point and that particular time [2]. The steady state solution is found as $\tau\to\infty$. There From Eq. (26), for the steady-state problems, after applying integral transforms on the developed governing equation for the time-invariant problems and their respective initial and boundary conditions, one arrives at

$$\tilde{\tilde{\theta}}(\beta_m,\bar{R})=\frac{Q_p}{2\pi\bar{R}}exp\left[-\beta_m\bar{R}\right]+\tilde{Q}'''_{work}+\tilde{1} \tag{42}$$

Application of inverse Fourier and Laplace transform to Eq. (42) gives

$$\theta(Z,\bar{R})=\frac{Q_p}{2\pi\sqrt{\left[(X-X')^2+(Y-Y')^2\right]}}\sum_{m=0}^{\infty}\frac{\begin{Bmatrix}(\beta_m^2+\beta_{bc}^2)[cos(\beta_m z)\\+Bi_{eff}sin(\beta_m z)]\end{Bmatrix}\begin{Bmatrix}exp\left\{-\beta_m\left[(X-X')^2+(Y-Y')^2\right]\right\}\\+\dfrac{2\pi\sqrt{\left[(X-X')^2+(Y-Y')^2\right]}}{Q_p}\dfrac{\tilde{Q}'''_{work}}{\beta_m{}^2}\end{Bmatrix}}{\left\{\left(\beta_m^2+Bi_{eff}^2\right)\left\{\left[(\beta_m^2+\beta_{bc}^2)+\beta_{bc}\right]+Bi_{eff}(\beta_m^2+\beta_{bc}^2)\right\}\right\}} \tag{43}$$

Where $\bar{R}\left(X,Y\right)=\left[(X-X')^2+(Y-Y')^2\right]$

As before, neglecting the heat generated in the slab or workpiece and assuming that the initial temperature of the workpiece is the same as the atmospheric, Eq. (43) reduces to

$$\theta(Z,\bar{R},\tau)=\frac{Q_p}{2\pi\left[(X-X')^2+(Y-Y')^2\right]}\sum_{m=0}^{\infty}\frac{\begin{Bmatrix}(\beta_m^2+\beta_{bc}^2)[cos(\beta_m Z)\\+Bi_{eff}sin(\beta_m Z)]\end{Bmatrix}\left\{exp\left\{-\beta_m\left[(X-X')^2+(Y-Y')^2\right]\right\}\right\}}{\left\{\left(\beta_m^2+Bi_{eff}^2\right)\left\{\left[(\beta_m^2+\beta_{bc}^2)+\beta_{bc}\right]+Bi_{eff}(\beta_m^2+\beta_{bc}^2)\right\}\right\}} \tag{44}$$

The above solutions in Eqs. (40) and (41) give the temperature at a point $P(X_, Y_, Z)$ at time τ in the infinite plate subjected to an instantaneous point moving heat source whose intensity is Q_p at point, $P(X_{o,} Y_{o,} 0)$ at time τ. When considering the moving point heat source, the total formation of the temperature distribution with respect to the distance from the moving point heat source at time τ is obtained by summing the respective contributions of all the instantaneous point moving heat sources for the time interval from $\tau'=0$ to $\tau'=\tau$ [26]. Then, the temperature distribution in the moving coordinate $(x_, y_, z)$ at time τ due to the heat input is given as

$$\theta(Z,\bar{R},\tau)=\frac{Q_p}{2\pi\sqrt{\left[X+X_o(\tau)-X_o(\tau')\right]^2+\left[Y-Y'\right]^2}}\left\{\begin{array}{l} exp\left\{-\left[\left(\dfrac{\left[X+X_o(\tau)-X_o(\tau')\right]^2+\left[Y-Y'\right]^2}{4(\tau-\tau')}\right)\right]\right\} \\ \times\displaystyle\sum_{m=0}^{\infty}\left\{\dfrac{\begin{Bmatrix}(\beta_m^2+\beta_{bc}^2)[cos(\beta_m z)\\+Bi_{eff}sin(\beta_m z)]\end{Bmatrix}\left\{\begin{array}{l} exp\left\{-\left[\left(\beta_m^2(\tau-\tau')\right)\right]\right\} \\ +\dfrac{2\pi\sqrt{\left[X+X_o(\tau)-X_o(\tau')\right]^2+\left[Y-Y'\right]^2}}{Q_p}\begin{Bmatrix}\dfrac{\tilde{Q}'''_{work}}{\beta_m^2}\left[1-exp(-\beta_m^2(\tau-\tau')\right] \\ +[\tilde{1}\times exp(-\beta_m^2(\tau-\tau')]\end{Bmatrix}\end{array}\right\}}{\left\{\left(\beta_m^2+Bi_{eff}^2\right)\left\{\left[(\beta_m^2+\beta_{bc}^2)+\beta_{bc}\right]+Bi_{eff}(\beta_m^2+\beta_{bc}^2)\right\}\right\}}\right\}\end{array}\right\} \tag{45}$$

Eq. (45) reduces to Eq. (46) if one neglects the heat generated in the slab and assumes that the initial temperature of the workpiece is the same as the atmospheric.

$$\theta(Z,\bar{R},\tau)=\frac{Q_p}{2\pi\sqrt{\left[X+X_o(\tau)-X_o(\tau')\right]^2+\left[Y-Y'\right]^2}}\left\{\begin{array}{l} exp\left\{-\left[\left(\dfrac{\left[X+X_o(\tau)-X_o(\tau')\right]^2+\left[Y-Y'\right]^2}{4(\tau-\tau')}\right)\right]\right\} \\ \times\displaystyle\sum_{m=0}^{\infty}\left\{\dfrac{\begin{Bmatrix}(\beta_m^2+\beta_{bc}^2)[cos(\beta_m z)\\+Bi_{eff}sin(\beta_m z)]\end{Bmatrix}\left\{\begin{array}{l} exp\left\{-\left[\left(\beta_m^2(\tau-\tau')\right)\right]\right\} \\ +\left(\dfrac{2\pi\sqrt{\left[X+X_o(\tau)-X_o(\tau')\right]^2+\left[Y-Y'\right]^2}}{Q_p}\right)\left\{[\tilde{1}\times exp(-\beta_m^2(\tau-\tau')]\right\}\end{array}\right\}}{\left\{\left(\beta_m^2+Bi_{eff}^2\right)\left\{\left[(\beta_m^2+\beta_{bc}^2)+\beta_{bc}\right]+Bi_{eff}(\beta_m^2+\beta_{bc}^2)\right\}\right\}}\right\}\end{array}\right\} \tag{46}$$

While for the steady state solution is found as $\tau\rightarrow\infty$.

$$\theta(Z,\bar{R}) = \frac{Q_p}{2\pi\sqrt{\left[X+X_o(\tau)-X_o(\tau')\right]^2+\left[Y-Y'\right]^2}}\sum_{m=0}^{\infty}\left\{\begin{array}{l}\left\{\begin{array}{l}(\beta_m^2+\beta_{bc}^2)[cos(\beta_m z)\\+Bi_{eff}\,sin(\beta_m z)]\end{array}\right\}\\ \times\dfrac{\left\{\begin{array}{l}exp\left\{-\beta_m\sqrt{\left[X+X_o(\tau)-X_o(\tau')\right]^2+\left[Y-Y'\right]^2}\right\}\\ +\dfrac{2\pi\sqrt{\left[X+X_o(\tau)-X_o(\tau')\right]^2+\left[Y-Y'\right]^2}}{Q_p}\dfrac{\tilde{Q}'''_{work}}{\beta_m{}^2}\end{array}\right\}}{\left\{\left(\beta_m^2+Bi_{eff}^2\right)\left\{\left[(\beta_m^2+\beta_{bc}^2)+\beta_{bc}\right]+Bi_{eff}(\beta_m^2+\beta_{bc}^2)\right\}\right\}}\end{array}\right\} \quad (47)$$

Therefore, for the case of neglected heat generated in the workpiece and when the workpiece maintains the same initial temperature as the atmospheric

$$\theta(Z,\bar{R}) = \frac{Q_p}{2\pi\sqrt{\left[X+X_o(\tau)-X_o(\tau')\right]^2+\left[Y-Y'\right]^2}}\sum_{m=0}^{\infty}\left\{\begin{array}{l}\left\{\begin{array}{l}(\beta_m^2+\beta_{bc}^2)[cos(\beta_m z)\\+Bi_{eff}\,sin(\beta_m z)]\end{array}\right\}\\ \times\dfrac{\left\{exp\left\{-\beta_m\sqrt{\left[X+X_o(\tau)-X_o(\tau')\right]^2+\left[Y-Y'\right]^2}\right\}\right\}}{\left\{\left(\beta_m^2+Bi_{eff}^2\right)\left\{\left[(\beta_m^2+\beta_{bc}^2)+\beta_{bc}\right]+Bi_{eff}(\beta_m^2+\beta_{bc}^2)\right\}\right\}}\end{array}\right\} \quad (48)$$

Where $X_o(\tau)=U\tau \; X_o(\tau')=U\tau'$

5 Results and Discussion

Figure (2) shows the variation of temperature with time at 2mm and 8 mm below the top surface and 8 mm and 16 mm from the centerline while Figure (3) shows the variation of temperature with time in the material at different depths and 8 mm from the centerline for a practical situation such as frictional stir welding of stainless steel.

The results show typical features of the temperature profiles in that the temperature rises rapidly and falls slowly toward advancing and retracting from a point. This is because as process proceeds, the heat source comes in contact with the cold slab and leaves behind a hot slab. Thereby, the temperature gradient ahead of the tool is high resulting in rapid heat transfer as compared to behind the tool.

Figure (4) depicts the variation of temperature with time at 16 mm below the top surface and 8 mm from the centerline while Figure (5) shows the variation of temperature with time in the material at different depths and 8 mm from the centerline for a practical situation such as frictional stir welding of aluminum. Figure (6) depicts the computed thermal cycles at several monitoring locations and depths. The locations are 4, 8, 12, and 16 mm below the top surface of the slab and at 8, 12, 16, and 20 mm from the heat source i.e. from the centerline.
The results show a rapid increase in temperature during heating followed by a comparatively slower cooling as the heat source moves away from the monitoring locations.

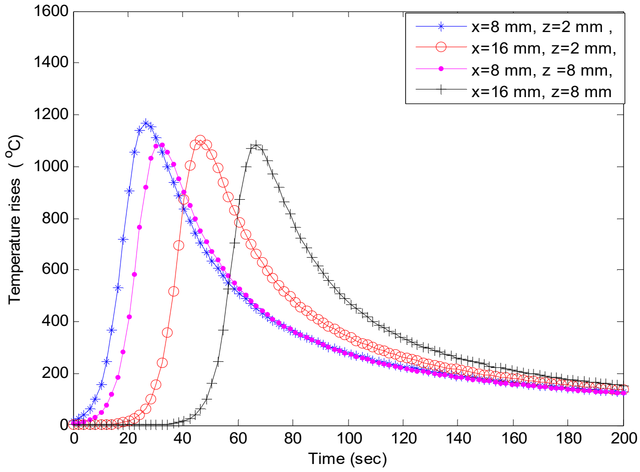

Figure 2 Temperature profiles in the material at 2mm and 8 mm below the top surface and 8 mm and 16 mm from the centerline.

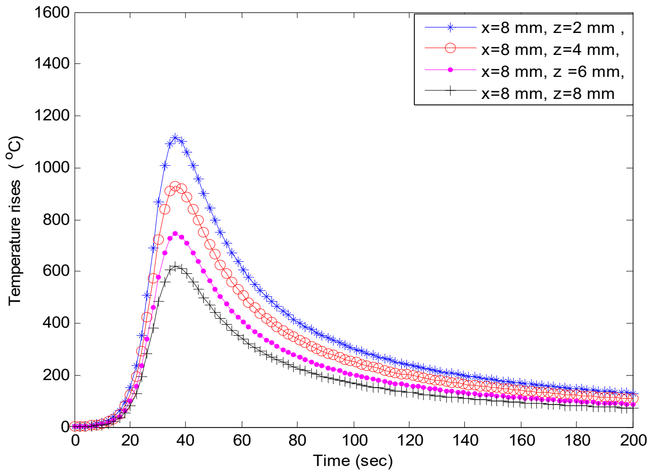

Figure 3 Temperature profiles in the material at different depths and 8 mm from the centerline.

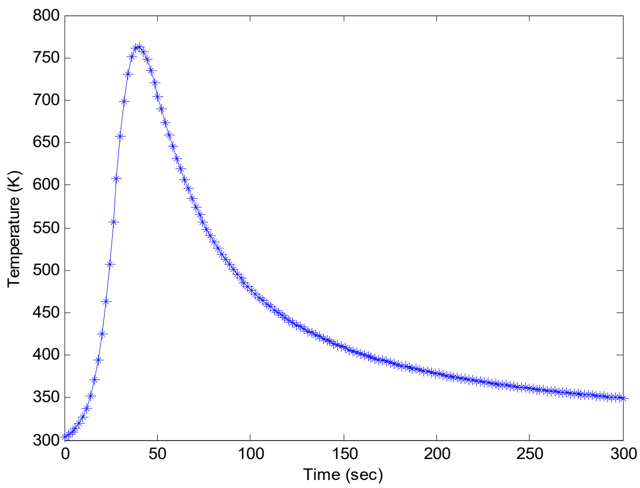

Figure 4 Variations temperature with welding time at x=8 mm and z=8 mm

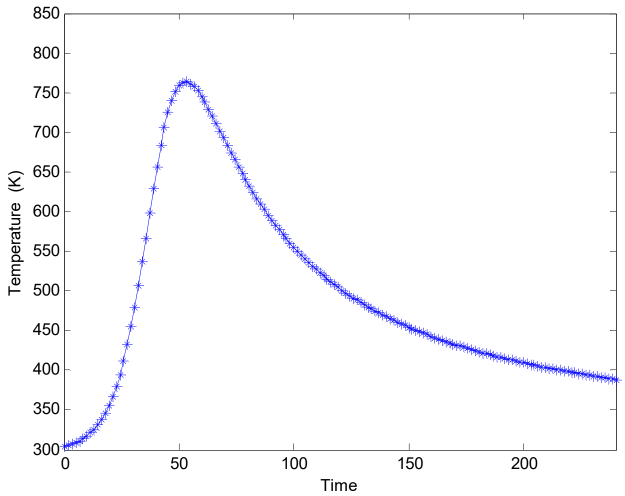

Figure 5 Variations temperature with welding time at x=8 mm and z=16 mm

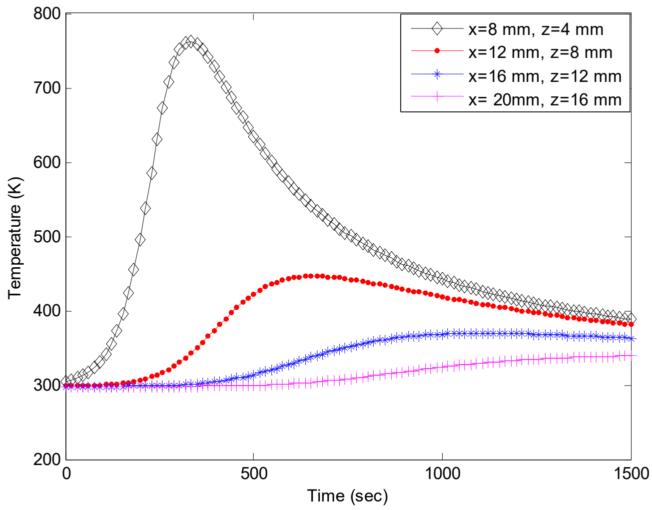

Figure 6 Temperature profiles in the material at different depths and different points from the centerline

Figures (7, 8) and (9) display the two dimensional temperature profiles in the moving heat source problem of aluminum alloy (AA-6061-T6) with the dimension of 300 x 200 x 16 mm. It could be seen that the curve bends backward. This is due to the finite time that it takes for heat to flow in materials, which delays the occurrence of the peak temperature at points along the y-axis. The shape of the curve depends on both the traverse speed and the thermal diffusivity of the material. The peak temperature at a given point is experienced by the point shortly after it is passed by the heat source. This is evident from an isotherm (locus of points with the same temperature) of the temperature distribution. At any position of the heat source, the isotherms of various temperatures are oval shaped. Higher temperatures have smaller size ovals.

The point on any isotherm that is furthest from the x-axis (or line of motion of the heat source) is at its peak temperature at that instant. The initial steep heating is observed as the monitoring locations encounter compressed thermal contours ahead of the heat source.

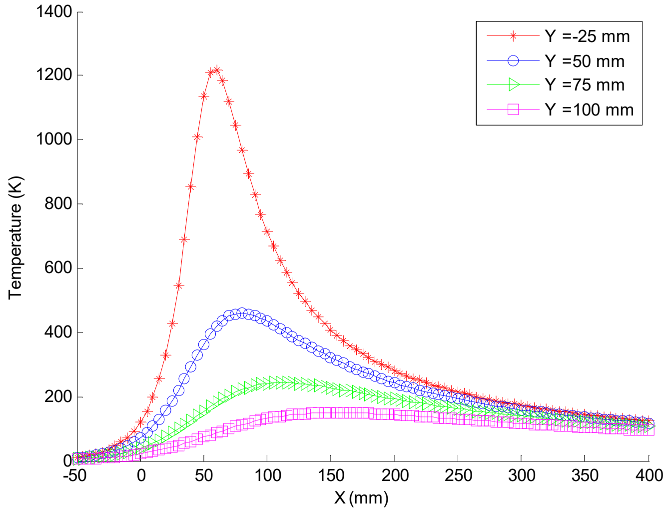

Figure 7 Temperature rise profiles without pre-heating along welding direction at different welding positions y

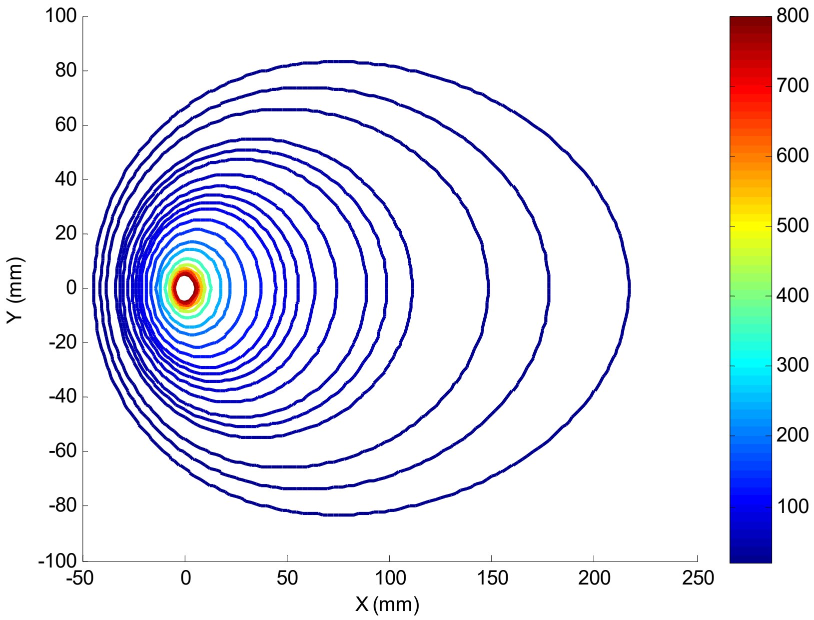

Figure 8 Temperature contour/profiles plot in x-y full-plane at x=0 mm with -50 mm from the edge

As the point heat source moves ahead of the monitoring locations, the expanded temperature contours lead to slow cooling. The higher the heat source velocity, the faster the temperature changes during both heating and cooling. The three dimensional plot that depicts peak temperature at the different locations in the material is shown in Figure (10) and (11) it is shown that increasing the initial workpiece temperature reduces the cooling rate, and is more effective than increasing the heat input or reducing the traverse velocity.

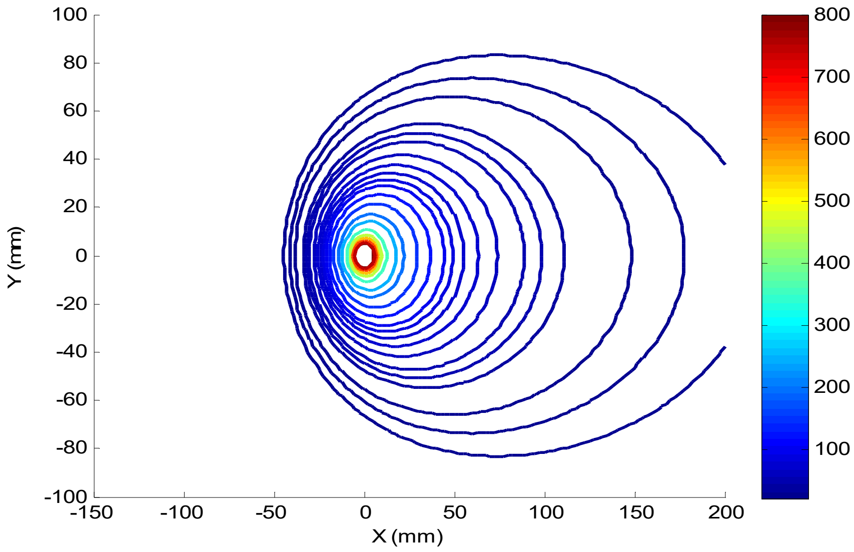

Figure 9 Temperature contour/profiles plot in x-y full-plane at x=0 mm with -150 mm from the edge

6 Conclusion

In this work, analysis of three-dimensional transient heat transfer in a moving heat source problem has been carried out using integral transforms methods. The computed results at different monitoring locations show typical features of the temperature profiles and they afford a close analysis of the factors governing the heat flow in a point moving heat source.
Therefore, the model can serve as benchmark for numerical solutions for the determination of temperature profiles in a point moving heat source problem.

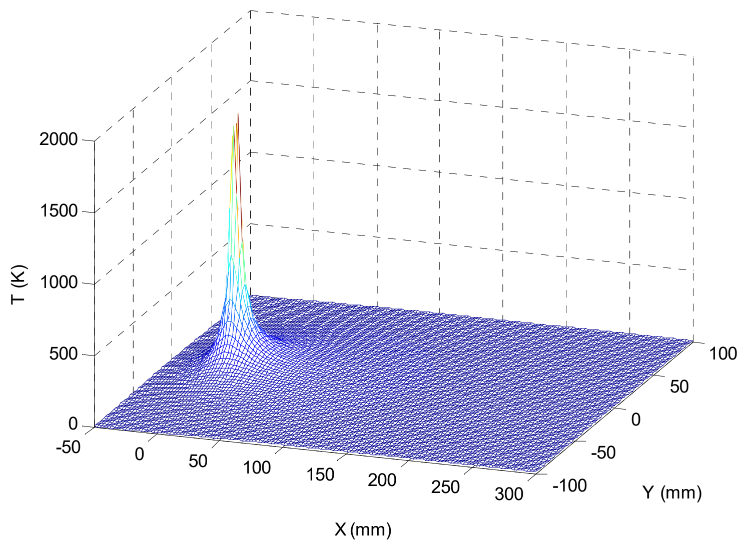

Figure 10 Three-dimensional D-plot Temperature rise profiles without pre-heating along welding direction

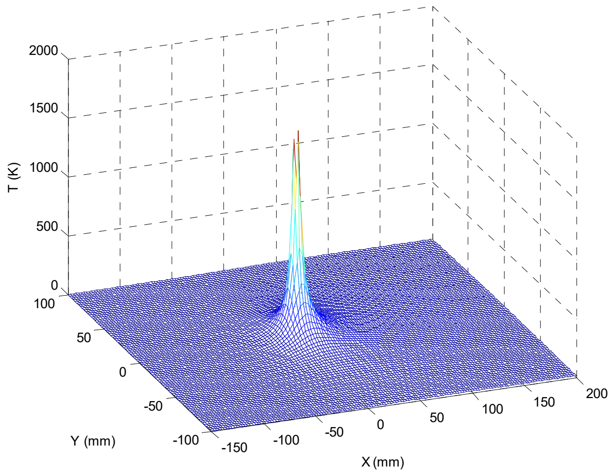

Figure 11 Three-dimensional D-plot Temperature rise profiles without pre-heating along welding direction

References

[1] Hou, Z. B., and Komanduri, R., "General Solutions for Stationary/Moving Plane Heat Source Problems in Manufacturing and Tribology", Int. J. Heat Mass Transfer, Vol. 43, No. 10, pp. 1679–1698, (2000).

[2] Dowden, J. M., Ducharme, R., and Kapadia, P. D., "Time-dependent Line and Point Sources: A Simple Model for Time-dependent Welding Processes", Lasers in Engineering, Vol. 7, No. 3-4, pp. 215-228, (1998).

[3] Rosenthal, D., and Carmern, R. H., "Temperature Distribution in Cylinder Heated by Point Source Moving Along Its Axis, Trans. ASME, Vol. 69, pp. 961-968, (1947).

[4] Rosenthal, D., "The Theory of Moving Source of Heat and its Application to Metal Treatments, Trans. ASME, Vol. 68, pp. 849-866, (1949).

[5] Weichert, R., and Schonert, K., "Temperature Distribution Produced by a Moving Heat Source, Mech. Appl. Math. XXXI. pp. 363-379, (1978).

[6] Kim, C. K., "An Analytical Solution to Heat Conduction with a Moving Heat Source", Journal of Mechanical Science and Technology, Vol. 25, No. 4, pp. 895-899, (2011).

[7] Carslaw, H. S., and Jaeger, J. C., "*Conduction of Heat in Solids*", Oxford University Press, Oxford, (1959).

[8] Malmuth, N. D., "Temperature Field of a Moving Point-source with Change of State", Int. J. Heat Mass Transfer, Vol. 19, pp. 349-354, (1976).

[9] Grosh, R. H., Trabant, E. A., and Hawkins, G. A., "Properties Heated by Moving Heat Source", Mech. Appl. Math., XIII, Vol. 2, pp. 160-167, (1955).

[10] Kuang, Z. B., and Atluri, S. N., "Temperature Field Due to a Moving Heat Source: A Moving Mesh Finite Element Analysis", Trans. ASME, Vol. 52, pp. 274-280, (1985).

[11] Webb, B. W., and Viskanta, R., "Analysis of Heat Transfer during Melting the Pure Metal from an Isothermal Vertical Wall, Num. Heat Transfer, Vol. 9, pp. 539-558, (1986).

[12] Jeager, J.C., "Moving Sources of Heat and Temperature at Sliding Contacts", Proceeding of Royal Society, New South Wales, Vol. 76, pp. 203-224, (1942).

[13] Peak, U., Gagliano, F. P., "Thermal Analysis of Laser Drilling Processes", IEEE J. of Quantum Electronics, Vol. 2, pp. 112-119, (1972).

[14] Zubair, S. M., and Chaudhry, M. A., "Temperature Solutions Due to Time-dependent Moving Line Heat Sources", Heat and Mass Transfer, Vol. 3, pp. 185-189, (1996).

[15] Terauchi, Y., and Nadano, H., "On Temperature Rise Caused by Moving Heat Sources", Bull of JSME, Vol. 27, No. 226, pp. 831-838, (1984).

[16] Muzychka, Y. S., and Yovanovich, M. M., "Thermal Resistance Models for Non-circular Moving Heat Sources on a Half Space", Journal of Heat Transfer, ASME Trans. Vol. 123, pp. 624-632, (2001).

[17] Kou, W. L., and Lin, J. F., "General Temperature Rise Solution for a Moving Plane Heat Source Problem in Surface Grinding", Int. J. Adv. Manuf. Technol. Vol. 31, pp. 268-277, (2006).

[18] Nguyen, N. T., Onta, A., Matsuoka, K., Suzuki, N., and Maeda, Y., "Analytical Solutions for Transient Temperature of Semi-Infinite Body Subjected to 3-D Moving Heat Sources", Supplement of Welding Research Journal, August, (1999).

[19] Zhang, H. J., "Non-quasi-steady Analysis of Heat Conduction from a Moving Heat Source", ASME J. Heat Transfer, Vol. 112, pp. 777-779, (1990).

[20] Tian, X., and Kennedy, F. E., "Maximum and Average Flash Temperature in Sliding Contacts", ASME J. Tribology, Vol. 116, pp. 167-174, (1994).

[21] Zeng, Z., Brown, M. B., and Vardy, V. E., "On Moving Heat Sources", Heat and Mass Transfer, Vol. 33, pp. 41-49, (1997).

[22] Levin, P., "A General Solution of 3-D Quasi-steady State Problem of a Moving Heat Source on a Semi-infinite Solid", Mech. Research Communication, Vol. 35, pp. 151-157, (2008).

[23] Yovanovich, M.M., "Transient Spreading Resistance of Arbitrary Isoflux Contact Areas: Development of a Universal Time Function", 33rd Annual AIAA Thermophysics Conference, (1997).

[24] Negus, K. J., and Yovanovich, M. M., "Transient Temperature Rise at Surface Due to Arbitrary Contacts on Half Space", Transaction of CSME, Vol. 13, No. 1/2, pp. 1-9, (1989).

[25] Akbari, M., Sinton, D., and Bahrami, M., "Moving Heat Sources in a Half Space: Effects of Source Geometry", Proceedings of the ASME 2009 Heat Transfer Summer Conference HT2009, San Francisco, California, USA, July 19-23, (2009).

[26] Jeong, S. K., and Cho, H. S., "An Analytical Solution for Transient Temperature Distribution in Fillet arc Welding Including the Effects of Molten Metal", Proceedings of the Institute of Mechanical Engineers, Part B: Journal of Engineering Manufacture, Vol. 211, pp. 63-72, (1997).

[27] Muzychka, Y. S., and Yovanovich, M. M., "Thermal Resistance Models for Non-circular Moving Heat Sources on a Half Space", ASME J. Heat Transfer, Vol. 123, No. 4, pp. 624–632, (2001).

[28] Terauchi, Y., Nadano, H., and Kohno, M., "On the Temperature Rise Caused by Moving Heat Sources. II: Calculation of Temperature Considering Heat Radiation from Surface", Bull. JSME, Vol. 28, No. 245, pp. 2789–2795, (1985).

[29] Yovanovich, M. M., Negus, K. J., and Thompson, J. C., "Transient Temperature Rise of Arbitrary Contacts with Uniform Flux by Surface Element Methods", Presented at the 22nd AIAA Aerospace Sciences Meeting, Reno, NV, Vol. 16, Jan 9–12, (1984).

[30] Eagar, T. W., and Tsai, N. S., "Temperature Fields Produced by Traveling Distributed Heat Sources", Weld. J., Miami, FL, U.S., Vol. 62, No. 12, pp. 346– 355, (1983).

[31] Yevtushenko, A. A., Ivanyk, E. G., and Ukhanska, O. M., "Transient Temperature of Local Moving Areas of Sliding Contact", Tribol. Int., Vol. 30, No. 3, pp. 209–214, (1997).

[32] Zubair, S. M., and Chaudhry, M. A., "A Unified Approach to Closed-form Solutions of Moving Heat-source Problems, Heat Mass Transfer, Vol. 33, No. 5–6, pp. 415–424, (1998).

[33] Baıri, A., "Analytical Model for Thermal Resistance Due to Multiple Moving Circular Contacts on a Coated Body", C. R. Mec., Vol. 331, No. 8, pp. 557–562, (2003).

[34] Bianco, N., Manca, O., Nardini, S., and Tamburrino, S., "Transient Heat Conduction in Solids Irradiated by a Moving Heat Source", Presented at the Proceedings of COMSOL Users Conference, Milan, (2006).

[35] Wen, J., and Khonsari, M. M., "Analytical Formulation for the Temperature Profile by Duhamel's Theorem in Bodies Subjected to an Oscillatory Heat Source", ASME J. Heat Transfer, Vol. 129, pp. 236–240, (2007).

[36] Manta, S., Nardini, S., and Naso, V., "Analytical Solution to the Temperature Distribution in a Finite Depth Solid with a Moving Heat Source", Proceedings of the 4th Brazilian Thermal Science Meeting, pp. 287-291, (1992).

[37] Modest, M.F., and Abakians, H., "Heat Conduction in a Moving Semi-infinite Solid Subjected to Pulsed Laser Irradiation", J. Heat Transfer. Vol. 108, pp. 597-601, (1986).

[38] Lolov, N., "Temperature Field with Distributed Moving Heat Source", International Institute of Welding, Study Group 212, Doc. 212-682-87, (1987).

[39] Manca, O., Morrone, B., and Naso, V., "Quasi-steadystate Three-dimensional Temperature Distribution Induced by a Moving Circular Gaussian Heat Source in Finite Depth Solid", Int. J. Heat Mass Transfer, Vol. 38, pp. 1305-1315, (1995).

Nomenclature

A_r Arbitrary selected area on the tool
Bi Biot number
Bi_{bc} Biot number at the base
Bi_{eff} Effective Biot number
c_p Heat capacity
H Height of the point heat source
k Thermal conductivity
Q Heat source surface area
$Q_{wor\,k}$ Rate of internal heat generation per unit volume of the slab/workpiece
R_p radius of the pin/inner radius of the point heat source
R_s radius of the shoulder/outer radius of the point heat source
$\dot{Q}_p$ internal heat generation by the pin in the tool
$\overline{R}$ dimensionless radius
T Temperature at any arbitrary point
$T\infty$ ambient temperature
v Heat source speed
V volume
θ dimensionless temperature
X, Y, Z dimensionless distances
τ dimensionless time
γ is the fraction of heat partitioned to the slab/workpiece.
σ Stefan-Boltmann constant
ε emmisivity
h_{eff} effective heat transfer coefficient
α Thermal diffusivity
ρ Density
β_b heat transfer coefficient at the base

چکیده

در این مقاله، انتقال حرارت گذرای سه بعدی در یک باریکه با منبع حرارتی داخلی که بوسیله یک منبع حرارتی نقطه‌ای متحرک در راستای طولش گرم می‌شود، با بکار گرفتن روش تبدیل انتگرالی مورد تحلیل قرار گرفته است. حرارت ورودی به باریکه یا قطعه کار توسط منبع حرارتی متحرک در مدل در نظر گرفته شده است. نتایج نشان می‌دهند که درجه حرارت ماده در طی مراحل انتقال حرارت کاهش پیدا می‌کند در حالی که زمان مورد نیاز برای رسیدن به ماکزیمم درجه حرارت با افزایش فاصله از خط مرکز، افزایش پیدا می‌کند.
همچنین نرخ حرارت و نرخ خنک شدن با افزایش فاصله از مرکز افزایش پیدا می‌کند. نتایج محاسبه شده در نقاط مختلف مورد بررسی نشان دهنده ویژگی های خاص پروفیل های درجه حرارت است و تحلیل نزدیکی از عوامل موثر بر جریان حرارتی در یک منبع حرارتی متحرک نقطه‌ای بدست می‌دهد.